Paper:

Evaluation of Seismic Vulnerability of Buildings Based on Damage Survey Data from the 2007 Pisco, Peru Earthquake

Shizuko Matsuzaki*, Nelson Pulido, Yoshihisa Maruyama*, Miguel Estrada***, Carlos Zavala***, and Fumio Yamazaki***

*Graduate School of Engineering, Chiba University
1-33 Yayoi-cho, Inage-ku, Chiba 263-8522, Japan
E-mail: matsu.shizuko@gmail.com
**National Research Institute for Earth Science and Disaster Prevention, Ibaraki, Japan
***Japan-Peru Center for Earthquake Engineering Research and Disaster Mitigation,
National University of Engineering, Lima, Peru
[Received July 30, 2014; accepted September 9, 2014]

The seismic vulnerability of buildings located in Pisco, Peru, was studied using damage survey data and seismic ground motion simulation. Inventory and damage information for more than 10,000 buildings was registered in survey data compiled by CISMID at Peru's National University of Engineering. The soil classes in the Pisco district were classified into three zones based on the predominant periods of microtremors at 85 sites, and damage ratios were calculated for each zone. Surface ground motions in each zone were estimated on the basis of base-rock motion simulation and shallow soil-column response analysis. Finally, fragility curves for adobe and brick masonry buildings were derived in terms of PGA and PGV. The results were compared with fragility functions developed in other studies.

Keywords: seismic vulnerability, the 2007 Pisco earthquake, building damage, damage survey

1. Introduction

The Pacific coast of South America is a segment of the circum-Pacific seismic belt along which a large number of thrust earthquakes have occurred [1]. Peru is located in an area of very high seismic activity. Buildings in different countries vary considerably in their materials and construction methods and thus in their seismic behavior. To assess earthquake-induced damage, it is necessary to consider the regional characteristics of buildings. For example, most mid-rise and low-rise buildings in provincial cities in Peru are constructed of bricks or adobe (air-dried mud brick) [2]. The patterns of collapse of such buildings are different from those of framed buildings. Residential buildings are built by local workers or by the inhabitants themselves, without sufficient knowledge of engineering. Because of inadequate financial resources, people buy construction materials little by little and add on to the buildings in which they live over the course of years [3].

The 2007 Pisco, Peru earthquake occurred off the coast of central Peru on August 15, 2007, at 18:40 local time (23:40 UTC). According to the United States Geological Survey (USGS), the earthquake had a moment magnitude of 8.0. The earthquake caused extensive damage to cities in Ica Region, including Pisco, Chincha, and Ica. Approximately 500 people were killed, and more than 90,000 buildings collapsed [4].

This study presents the results of an assessment of the seismic vulnerability of buildings located in Pisco, Peru, conducted using damage survey data and simulated seismic ground motions. Fragility curves for adobe and brick masonry buildings were constructed based on the results. Fragility curves are widely used to predict building damage due to earthquakes. Fragility curves have been developed in other studies from statistical analyses of actual damage data [5–7] and analyses of the seismic capacity of buildings [8–11]. To reflect regional seismic characteristics appropriately in damage assessment, it is necessary to confirm the validity of the damage evaluation methodology used. Hence, the fragility curves developed in this study were compared with curves developed in other studies.

2. Damage to Buildings in Pisco, Peru as a Result of the 2007 Earthquake

2.1. Breakdown of Building Types from Damage Survey Results

The District of Pisco is the capital of Pisco Province, which belongs to the Ica Region of Peru. The district is approximately 250 km south of Lima, the capital of Peru. The size of the main urban area of Pisco is about 2 km^2. Pisco faces the Pacific Ocean and has a desert climate. According to Peru's National Institute of Statistics and Information (INEI), the urban population was estimated to be 55,000 in 2007 [12]. The district is located 10 to 30 m above sea level and has a few topographic undulations. The Pisco River runs 2 km north of the town, and there

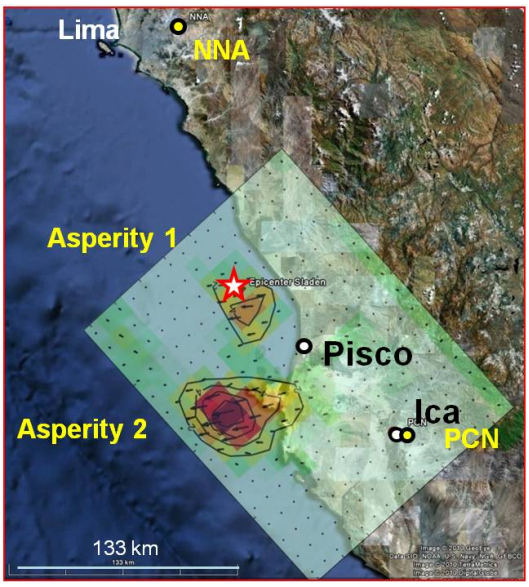

Fig. 1. Slip distribution of the 2007 Pisco, Peru earthquake from source process by Sladen et al. [13].

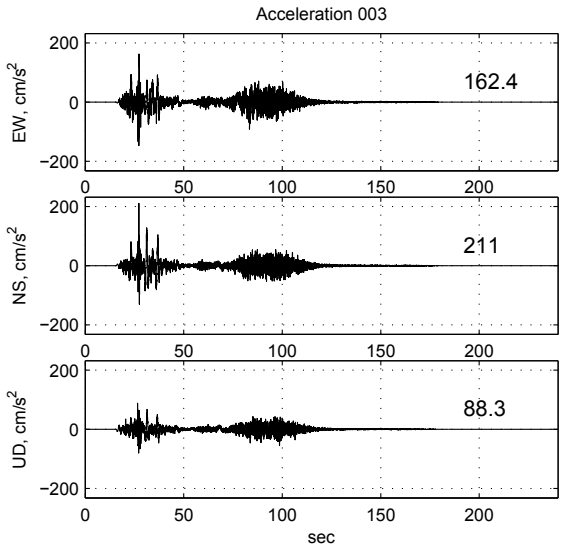

Fig. 2. Simulated bedrock accelerations at city center of Pisco.

are some marshes in the northern part of the town and near the coast. The Pisco district was the district most severely affected by the August 15, 2007 earthquake, which had a Modified Mercalli Intensity (MMI) of IX (USGS).

Ground motion records were not obtained in Pisco and nearby Chincha during this earthquake. Ground motions were recorded in Lima and Ica and at the Parcona station (PCN) in the Ica region. **Fig. 1** shows a slip model of the seismic source, and **Fig. 2** shows simulated bedrock accelerations at the city center of Pisco [14]. The records from Lima and Ica both consist of two distinct sub-events. At PCN, a peak ground acceleration of 484 cm/s^2 was recorded.

The present authors investigated the building damage situation soon after the earthquake. A field survey was conducted by the Japan–Peru Center for Earthquake Engineering Research and Disaster Mitigation (CISMID) in the National University of Engineering (UNI). A total of 12,000 building lots in the Pisco district were surveyed. The occupancy category, number of stories, structural type, and damage level were recorded for 10,480 building lots. Building damage was analyzed statistically by Zavala et al. [15] and Matsuzaki et al. [16]. More than 40 investigators were employed to conduct the field survey, which took almost three months to complete.

According to the survey, most of the structures were low-rise buildings; 72% were one-story buildings, and 23% were two-story buildings. The tallest building, which was six stories, was used as a hotel. Of the brick masonry buildings, 65% were one story, 29% were two stories, 5.3% were three stories, and 0.4% were four or more stories. Of the adobe buildings, in contrast, 99% were one story. Overall, the central part of Pisco district was found to be densely built-up with low-rise buildings. Roofs were mostly flat; roof tile was not typically used because of the desert climate of the region. In terms of building occupancy, 75% were residential, 7% were commercial, and the others were schools, hospitals, factories, and buildings used for other purposes.

Most of the buildings in Pisco were masonry: 16% were adobe masonry, and 71% were burned brick masonry. The other 13% were reinforced concrete (RC), Quincha, or mixed structures. Adobe houses can be found in almost every part of the world; however, their construction methods and seismic performance vary from region to region. In the rural areas of Peru, adobe blocks are typically made by buildings' inhabitants, and in urban areas, ready-made adobe blocks are sold at do-it-yourself home centers. Quincha (a Kechua word pronounced "kincha") is a type of construction that is traditional in South America and employs panels supported by wooden frames and cane-and-mud walls [17]. A few of the RC buildings surveyed were commercial buildings, such as banks and small hotels.

In Peru, the national building seismic code covers both brick masonry (under E.070) and adobe structures (under E.080) [18]. Most Peruvian brick masonry structures are known as confined masonry. These structures have relatively high horizontal stiffness because concrete slabs and RC columns and beams are often used. The cross-sectional areas of the RC columns are usually greater than 25 cm^2, unlike RC columns used for similar purposes in other countries, such as Indonesia [3]. On the other hand, adobe structures with mud-and-bamboo roofs are highly vulnerable to earthquakes [2].

2.2. Extent of Building Damage

During the survey, building damage levels were classified into four grades, namely, No damage, Slight damage, Moderate damage, and Severe damage. The definitions of the damage levels and their relationship to the European Macroseismic Scale (EMS) 1998 [19] damage categories are shown in **Table 1**. Slight damage is manifested as repairable small cracks on the finishing walls. Severe dam-

Table 1. Description of damage classifications used in the survey by CISMID and corresponding damage levels in EMS 1998.

Damage classification used in Peru		EMS 1998
	No damage No damage or Very slight damage.	G1
	Slight Cracks on walls but not structural damage. Completely reparable.	G2
	Moderate Structural damage. Possibility of retrofitting or relocation, require evaluation by expert.	G3
	Severe, Collapse Not usable or Collapse. Lowermost story collapse.	G4,G5

age includes collapse, which means that walls and roofs have partially or completely fallen down. Moderate damage covers structural damage, which needs evaluation by an expert to establish retrofitting needs. This classification system was originally developed by CISMID on the basis of local structural characteristics. The system is well known in Peru and is widely accepted among decision makers, researchers, professors, and people involved in building construction. **Fig. 3** shows the damage distribution for the adobe buildings surveyed, and **Fig. 4** shows the damage distribution for the brick masonry buildings.

Figure 5(a) and **Table 2** show the number of damaged buildings' lots and the damage ratios by structural type. The total number of buildings' lots whose structural types could be identified was 10,480. "Other" structure types in the figure and table were Quincha, mixed, or other structure types. An example of a mixed structure is a mixture of adobe and Quincha. The proportion of all of the buildings' lots that collapsed or suffered fatal (classified as severe) damage was 27%, and the combined proportion of moderate and severe damage was 40%. The degree of earthquake-induced damage observed depends on the characteristics of masonry structures, specifically their lack of rigidity, which makes them prone to collapse.

Adobe is quite vulnerable to earthquake damage. In this study, 83% of the adobe structures surveyed had severe damage. Although adobe buildings make up no more than 17% of all buildings in the district, 1,543 of the 2,779 lots (56%) that suffered severe damage were adobe.

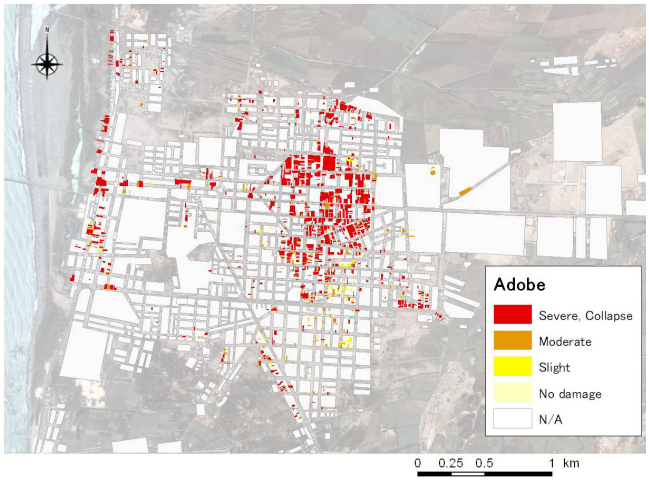

Fig. 3. Damage distribution of 1,865 lots of adobe buildings. Adobe buildings were found largely in the old urban area of the Pisco district.

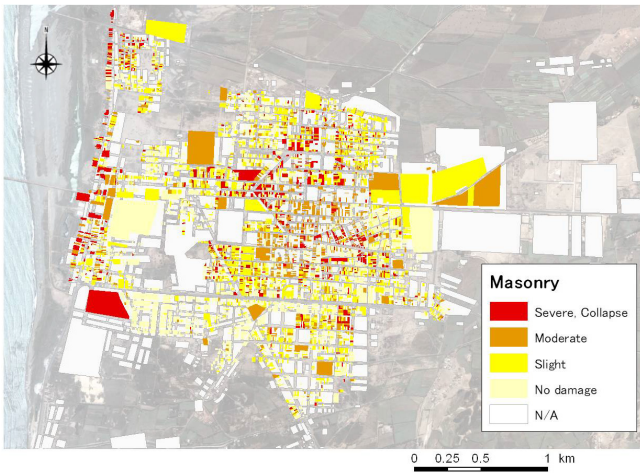

Fig. 4. Damage distribution of 8,298 lots of masonry buildings.

The severe damage ratio for concrete buildings was also high (22%). The severely damaged concrete structures were assumed to be pre-code buildings and/or to have been constructed without the involvement of professional engineers.

Figure 5(b) and **Table 3** show the damage ratios for masonry buildings with respect to the number of stories. In general, the greater the number of stories was, the heavier the damage was. However, for one-story buildings, the ratio of severe damage was rather high (17.2%) and in fact greater than that for two-story buildings (4.8%). For masonry buildings, the degree of damage observed was not related to the building occupancy (use) or the natural period. With regard to the occupancy, there were no significant differences between one-story and two-story buildings. In the case of one-story buildings, 89% were residential, and 8% were commercial. In the case of two-story buildings, 87% were residential, and 10% were commercial. Assuming that the natural period of a brick masonry building with an RC frame is proportional to the number of stories, with a coefficient of 0.08, the natural period of

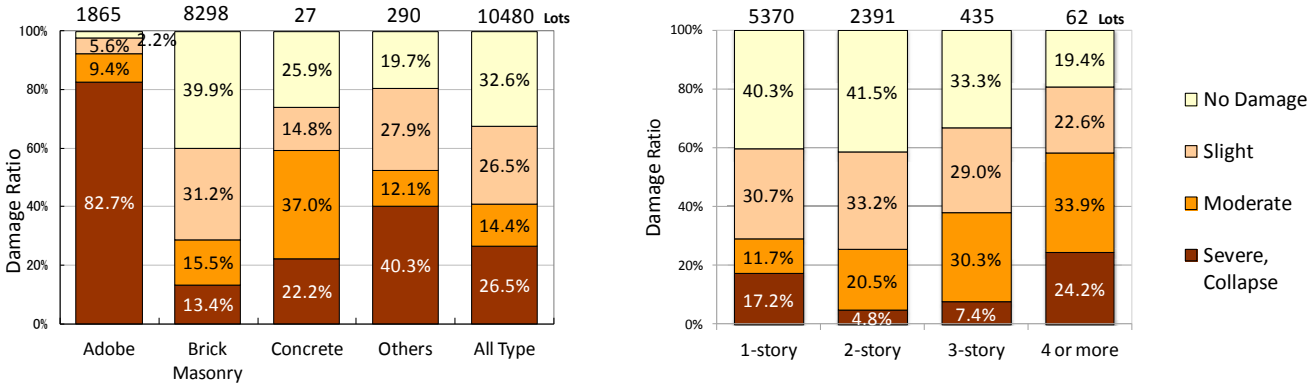

(a) Damage by structural type

(b) Masonry damage by number of stories

Fig. 5. (a) Building damage ratio by structure type and (b) damage ratio of masonry buildings by number of stories.

Table 2. Number of damaged building lots by structure type.

	Adobe	Brick masonry	Concrete	Others	Total
No damage	41	3,315	7	57	3,420
Slight	105	2,586	4	81	2,776
Moderate	176	1,284	10	35	1,505
Severe, Collapse	1,543	1,113	6	117	2,779
Total (Lots)	1,865	8,298	27	290	10,480

Table 3. Number of damaged building lots by number of stories for 8252 brick masonry buildings.

	1-story	2-story	3-story	4 or more	Total
No damage	2,165	993	145	12	3,315
Slight	1,651	794	126	14	2,585
Moderate	631	490	132	21	1,274
Severe, Collapse	923	114	32	15	1,084
Total (Lots)	5,370	2,391	435	62	8,258

two-story buildings is around 0.16 s, and that of a one-story building is less than 0.10 s. Because the predominant periods of the acceleration response spectra of the simulated bedrock motion were between 0.2 s and 1.0 s, resonance was not the cause of the damage observed in the one-story buildings.

Other factors in the amount of damage seen may be the structural specifications of masonry buildings. In general, two-story masonry buildings in Peru have reinforcement members, such as RC beams and columns, and concrete slabs, and thus they have a certain amount of seismic resistance. On the other hand, some one-story masonry buildings are not reinforced with RC members. In the construction of confined masonry buildings, walls are often constructed prior to columns, and hence the bond strength between brick walls and columns is great. Thus, RC column members can transmit their seismic resistance to foundations [20].

Besides, RC slabs do increase floor rigidity, and hence all the walls of a given story bear the shear force on that story. Consequently, the seismic capacity of the building as a whole is increased. **Fig. 6(a)** shows the exterior of a reinforced masonry building in Peru for which some columns and an RC slab can be seen. **Fig. 6(b)** shows an indoor view of an unreinforced masonry building without RC elements. The walls are made of bricks, but the roof is made of bamboo covered by mud.

Figure 7 shows the spatial distribution of damage ratios for masonry buildings with moderate or severe damage or collapse, with respect to the city block. The Pisco district was divided into 183 blocks, each of which had at least 30 masonry buildings. Regional differences are evident in the damage ratios: significant damage occurred in the area along the coast and in the old urban area near the main square, as also shown in [21]. The ages of the buildings are unknown; however, masonry buildings do not suffer from degradation over time due to decay or ants, unlike wooden Japanese houses [22]. Differences in ground motion intensity due to soil differences are believed to be among the reasons for the differences observed in the damage distribution.

3. Microzoning and Seismic Ground Motions

3.1. Seismic Microzoning Using Microtremors

According to the results of several standard penetration tests (SPTs) conducted by CISMID, hard soil with gravel

(a) Reinforced brick masonry (RM)

(b) Unreinforced brick masonry (URM)

Fig. 6. (a) Exterior view of reinforced masonry building with RC frame in Peru and (b) indoor damage state of one-story unreinforced masonry (URM) building without RC elements. The URM building has a roof of bamboo covered by mud.

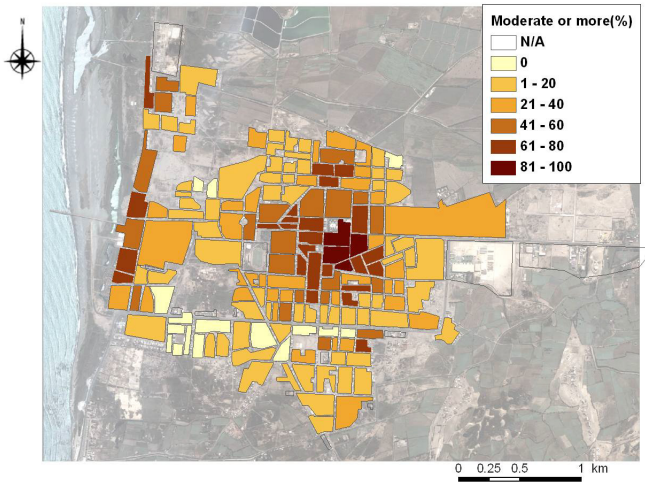

Fig. 7. Spatial distribution of moderate or greater damage ratio for masonry buildings by city block. Each block was divided to include at least 30 masonry buildings.

can be found around the Pisco district below the shallow surface soil layer. Near the coast, the groundwater table is high, and liquefaction due to the earthquake was observed. From 2007 to 2011, CISMID and Johansson et al. conducted microtremor measurements at 73 sites in the Pisco area [23]. In 2012, 12 new sites, including three at which array measurements were conducted, were added to the set of microtremor measurement sites.

Nakamura proposed that the H/V (horizontal-to- vertical) spectral ratio of microtremors could be considered the spectral amplification ratio of subsurface soil layers at a given site [24, 25]. **Fig. 8** shows the locations of the 85 sites at which microtremor measurements were made, along with peak periods of the H/V spectra and the spatially interpolated H/V peak periods. Using the inverse distance-weighted method [26], interpolation of the peak periods was performed by averaging the data from 12 nearby points. The target area was divided into three zones, 1 to 3. Darker colors indicate longer peak periods of the sites.

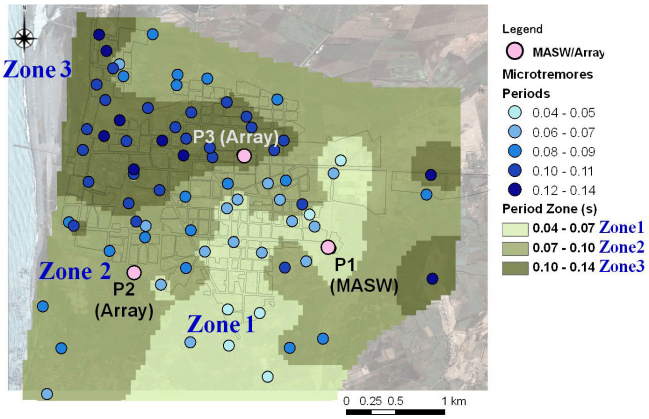

Fig. 8. Location of three MASW/array measurements and results of spatial interpolation of H/V ratio of single-point microtremor for 85 peak periods, using the inverse distance weighted method.

The ground was estimated to be firm if the peak period of the H/V ratio was less than 0.1 s. The peak period of Zone 1 was between 0.04 and 0.07 s, that of Zone 2 was between 0.07 and 0.10 s, and that of Zone 3 was between 0.10 and 0.14 s. The northwestern part of the area is classified as relatively soft ground (Zone 3), and the southeastern part is firm ground (Zone 1).

Following the microzoning based on microtremors, the damage ratios shown in **Fig. 9** for adobe and brick masonry buildings were obtained. For 8,298 lots of masonry buildings, the damage ratios for both severe damage and moderate or greater damage were higher for softer soils (from Zone 1 to Zone 3). Similarly, for 1,865 lots of adobe buildings, firmer soils had lower damage ratios for all damage levels. The building damage ratio appears to be related to the soil classification through the peak period of the H/V ratio of microtremors, for both adobe and masonry structures in Pisco.

3.2. One-Dimensional Soil Response Analysis Using Simulated Bedrock Motion

Using synthetic aperture radar (SAR) interferometry data and teleseismic waveforms, the source model for the Pisco earthquake was constructed to reproduce the near-source strong ground motion recordings measured at the Nana (NNA) and PCN stations and shown in **Fig. 1**. The earthquake motions at the depth of the seismic bedrock ($V_s = 3,260$ m/s) were obtained by numerical simulation [14].

To estimate the seismic ground motions during the Pisco earthquake, the soil profiles at points P1, P2, and P3 in the three zones, shown in **Fig. 8**, were used. Multichannel analysis of surface waves (MASW) of the P1 site data, measured in relatively firm soil, was carried out in 2007. Array microtremor measurements were also carried out in 2012 at the P2 and P3 sites, in moderately soft and soft soils. The shear-wave velocity profiles at the three sites, up to GL-1,200 m, were estimated from an inversion between the phase velocity and the period, as shown

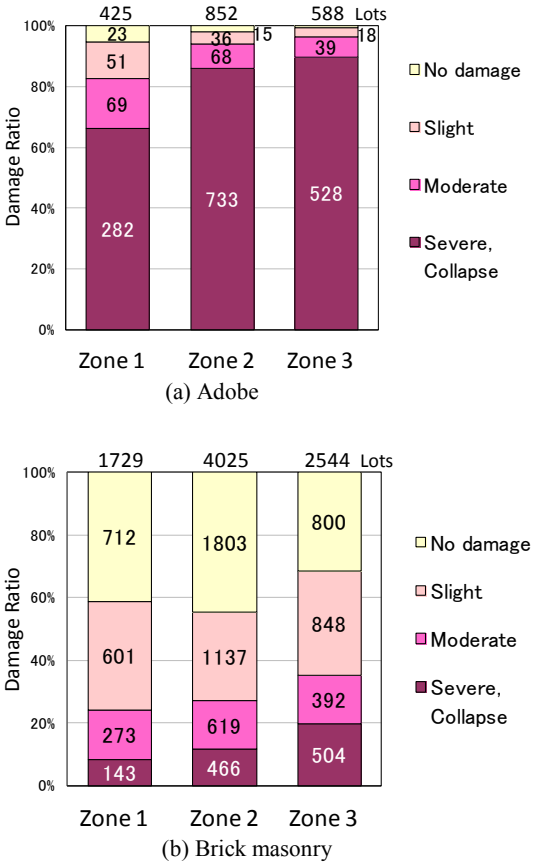

Fig. 9. Damage ratios by soil zone classification for (a) adobe buildings and (b) brick masonry buildings.

in **Fig. 10**. The soil profiles at the three sites were assumed to have a common soil structure at depths greater than GL-400 m.

The transfer functions and ground motions at the surface were derived from the results of a one-dimensional layered soil response analysis conducted using EERA, which is a version of the SHAKE program for Microsoft Excel developed by Bardet et al. [27]. Using as input the ground motion simulated by Pulido et al. (2013) at the outcrop base rock, one-dimensional (1D) equivalent linear seismic response analyses were performed. Strain-dependent nonlinearity of the soil was considered only for the uppermost layer. The clay model in EERA was used as the material type for the stress–strain and damping–strain curves. The default value for clay [28] was used for the modulus of the top layer. The ratio of the effective to the maximum shear strain was assumed to be 0.65.

The predominant periods of the transfer functions were approximately 0.07 s for P1 (Zone 1), 0.21 s for P2 (Zone 2), and 0.23 s for P3 (Zone 3). The simulated bedrock motions were available for these three points. The maximum ground surface acceleration and velocity (PGA and PGV) for each zone are summarized in **Table 4**. The resultant of the two horizontal components was also obtained for the three locations.

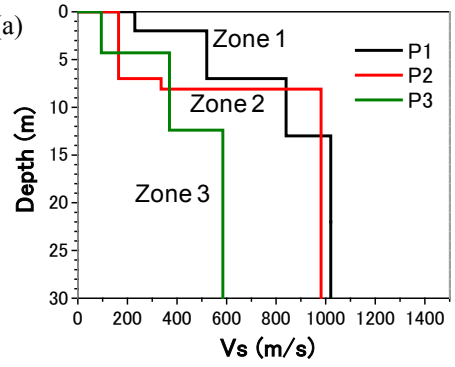

(b)

P1 (Zone 1)		P2 (Zone 2)		P3 (Zone 3)	
Depth (m)	Vs (m/s)	Depth (m)	Vs (m/s)	Depth (m)	Vs (m/s)
0 - 2	230	0 - 7	164	0 - 4	95
2 - 7	520			4 - 12	370
7 - 13	840	7 - 8	336	12 - 200	585
13 - 400	1020	8 - 400	981	200 - 400	700
400 - 700	1500	400 - 700	1500	400 - 700	1500
700 - 1200	2600	700 - 1200	2600	700 - 1200	2600
1200 - ∞	3260	1200 - ∞	3260	1200 - ∞	3260

Fig. 10. (a) Comparison of shear-wave velocity profiles among three measurement sites, P1 (Zone 1), P2 (Zone 2), and P3 (Zone 3), up to GL-30 m, and (b) up to GL-3,000 m.

Table 4. Maximum ground surface acceleration and velocity from one-dimensional response analysis for three zones.

	Site	EW	NS	Resultant vector
PGA (cm/s^2)	Zone 1 (Hard)	331.9	441.6	552.4
	Zone 2	523.0	365.8	554.4
	Zone 3 (Soft)	576.9	461.2	611.1
PGV (cm/s)	Zone 1 (Hard)	60.4	75.9	94.4
	Zone 2	64.1	81.0	99.5
	Zone 3 (Soft)	84.7	94.3	113.8

4. Development of Fragility Curves and Comparison with Curves from Previous Studies

4.1. Development of Fragility Curves

Fragility curves for adobe and masonry structures were constructed from the relationship between the damage ratio and the peak ground motion values (PGA and PGV). Assuming a log-normal distribution for the probability of damage occurrence greater than or equal to rank R, the cumulative probability $P_R(x)$ for a peak ground motion value x is expressed by the following equation:

$$P_R(x) = \Phi\left((\ln x - \lambda)/\zeta\right) \quad (1)$$

where Φ is the standard normal distribution and λ and ζ are the logarithmic mean and logarithmic standard deviation of $\ln x$, respectively. The values of these terms were obtained by regression analysis using log-normal probability paper.

Table 5. Coefficients of fragility curves for adobe and masonry buildings in Pisco.

Damage Grade		PGA			PGV		
		λ	ζ	R^2	λ	ζ	R^2
Adobe	Moderate or greater	-0.785	0.171	0.559	4.280	0.242	0.787
	Severe, Collapse	-0.710	0.184	0.490	4.393	0.253	0.727
Masonry	Moderate or greater	-0.413	0.223	0.614	4.828	0.355	0.608
	Severe, Collapse	-0.285	0.223	0.898	5.033	0.355	0.994

The results of the regression analysis are shown in **Table 5**. According to **Fig. 9(b)**, the damage ratios associated with slight or greater damage in Zone 1 were higher than those in Zone 2, while the PGA and PGV in Zone 1 were smaller than those in Zone 2. Therefore, a reasonable fragility function for slight or greater damage was not obtained in this study. As the regression for moderate or greater damage for masonry buildings had significant variation in the data around the regression line, the ζ value obtained for the severe damage state was assumed for this damage state as well.

4.2. Comparison of Fragility Curves for Adobe Buildings

The fragility curves obtained as described above were compared with fragility curves obtained in previous studies in terms of PGA using the capacity spectrum method. The curves developed in previous studies applied to typical building types in a particular country or region. In addition, the demand spectrum for each case was the one for an assumed earthquake scenario. In the previous development of fragility curves, the spectral displacement (S_d) or the spectral acceleration (S_a) was often used as an intensity measure, rather than the MMI seismic intensity or the PGA.

Tarque et al. derived fragility curves for one-story adobe dwellings in Cusco, Peru [9] as a function of PGA, based on an acceleration response spectrum for a seismic motion scenario. The fragility curves for conditions denoted by LS4 (near collapse or collapse) and LS3 (life-safety) were considered to correspond to the severe damage and moderate or greater damage levels, respectively, in the present study.

Figure 11 shows a comparison between the curves for Cusco and Pisco. The comparison suggests that the fragility curves for adobe in Pisco are similar to those for adobe in Cuzco, especially for the severe damage level. The damage ratio for Pisco is slightly lower than that of Cuzco, but the slope of the curve is steep. For both curves, the damage ratios for moderate or greater damage exceed 90% for PGA values of 0.6 g. The seismic performance of adobe buildings in Cuzco, as evaluated by Tarque et al. [9], is similar to that observed in this study.

4.3. Comparison of Fragility Curves for Masonry Buildings

The fragility curves for brick masonry structures in Pisco were compared with those for RM2L lifeline buildings in HAZUS and URM (unreinforced masonry) in Istanbul (developed by Erberik [10, 11]), as shown in **Fig. 12**. It is reasonable to assume that pre-code buildings in HAZUS correspond to non-conforming buildings under the present Peruvian building code regulations.

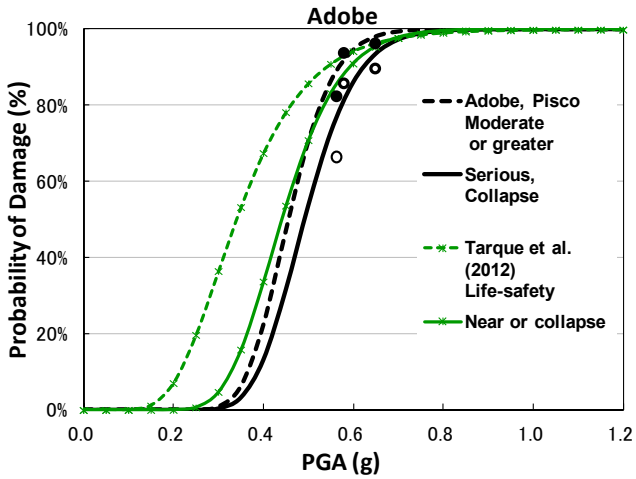

Fig. 11. Comparisonoffragilitycurvesobtainedinthisstudy-for buildings in Pisco with those obtained by Tarque et al. [9] for buildings in Cusco.

HAZUS-MH MR3 [8] is a standard multi-hazard tool for loss estimation due to seismic motion and ground failure for buildings, transportation systems, and lifeline facilities. The fragility curves of lifeline buildings are expressed as a function of an equivalent PGA. From among the lifeline building types, the low-rise RM2L (one- to three-story reinforced masonry bearing walls with precast concrete diaphragms) was selected for comparison, based on its similarity to the types of building structures found in Pisco. However, it is not as clear whether masonry bearing walls in HAZUS are similar to certain types of structures found in Peru, such as confined masonry buildings. "Masonry" refers broadly to a construction method based on layers using stone, brick, concrete block (CB), etc. The category of masonry includes various types of structures, such as brick masonry reinforced with a light-gauge steel frame [29]. The results of the comparison suggest that the brick masonry buildings in Pisco are much more vulnerable than RM2L buildings in HAZUS. This may be because HAZUS deals with other structural specifications than those considered in this study. As described previously, masonry buildings in HAZUS might include not only brick masonry but also CB.

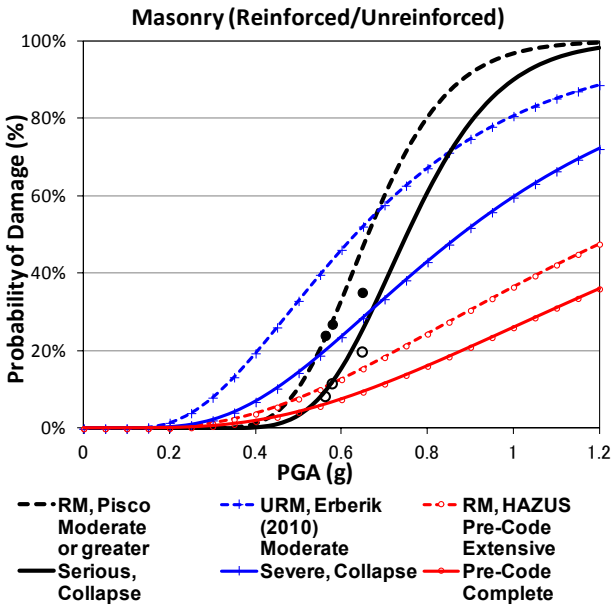

Fig. 12. Comparison of fragility curves (RM) for one- to two-story reinforced brick masonry buildings in Pisco with those (RM2L) for one- to three-story reinforced masonry bearing walls with precast concrete diaphragms in lifeline buildings in HAZUS [8] and those (URM) for one-story unreinforced regular buildings with solid brick walls in Istanbul obtained by Erberik [10, 11].

The study by Erberik [10, 11] addressed one-story unreinforced brick buildings with well-formed plans in Istanbul, Turkey. The brick masonry buildings considered in the present study were mainly one- to three-story buildings, and the two structural types are different. With respect to materials, brick masonry buildings in Istanbul are made of solid brick, whereas in Pisco, the walls on the second floor of a brick masonry building are made of perforated brick, and those on the ground floor are made of solid brick. Compared to the fragility curves for brick masonry in Istanbul, the fragility curves developed in this study indicate that the damage that occurs in confined masonry in Pisco (in one- and two-story buildings) starts to occur at a larger PGA value than in one-story unreinforced masonry in Istanbul but exhibits higher damage ratios at larger PGA values. The slopes of the fragility curves developed in this study were steeper than those developed in previous studies. The damage ratios for masonry buildings after the Pisco earthquake were smaller than those estimated using the fragility functions developed by Erberik [10, 11].

The results of the comparison of the damage ratios for structural types in Pisco indicate that more than 80% of adobe buildings suffered severe damage at a PGA of 0.6 g. The damage ratio for masonry buildings, for the same seismic excitation level, was 15%. The two fragility curves exhibit a clear difference in performance by structural type. The slopes of the adobe fragility curves are steeper than those of the masonry fragility curves, which suggests that just a small increase in the ground motion will result in serious damage in adobe. In other words, for adobe, the difference between the ground motion that produces moderate or greater damage and the ground motion that produces severe damage is small. This observation is consistent with the fact that adobe buildings are likely to exhibit significant damage suddenly and suffer brittle failure.

5. Conclusions

In this study, relationships between peak ground motion indices and building damage caused by the 2007 Pisco, Peru earthquake were investigated using damage survey data collected in the Pisco district and simulated ground motion records. Approximately 80% of the adobe buildings in the survey area suffered from serious damage, such as collapse, as a result of the earthquake. In contrast, the ratio of serious damage for brick masonry buildings was only approximately 13%. The extent of the damage observed varied widely, depending on the structural properties of the buildings surveyed, such as the presence or absence of concrete reinforcing members.

The subsurface soils in the area of Pisco were divided into three zones based on the predominant periods of microtremors measured at 85 sites. The relationship between a site's ground conditions and the damage ratio for each zone was confirmed. Compared to fragility functions derived by analytical methods in previous studies, the means and standard deviations for adobe structures in Pisco were quite similar to those for structures in Cusco. For brick masonry, the means in Istanbul and Pisco were similar, but within the range of ground motion of the Pisco earthquake (0.56 to 0.65 g), the damage ratio in Istanbul was 20% larger than in Pisco.

The damage survey conducted in Pisco covered a small area of only 2 km^2. The estimated ground motions exhibited no significant differences. It would be preferable to verify the reliability of the damage ratios determined using data from lower-damage-ratio areas for adobe structures and data from higher-damage-ratio areas for masonry buildings. In this study, one-story brick masonry buildings in Pisco were found to be a mixture of good and poor structures in terms of their seismic performance. Through a detail survey of floor specifications and with information on the proportion of unreinforced buildings, it might be possible to further validate the relationship between the structure type and degree of damage.

Acknowledgements

The authors are grateful to Prof. Hiroaki Yamanaka and Dr. Kosuke Chimoto of the Tokyo Institute of Technology and Mr. Fernando Lazares of UNI for their support during the array measurements in Pisco.

References:

[1] F. Yamazaki and C. Zavala, "SATREPS project on enhancement of earthquake and tsunami disaster mitigation technology in Peru," Journal of Disaster Research, Vol.8, No.2, pp. 224-234, 2013.

[2] M. Blondet, J. Vargas, and N. Tarque, "Observed behaviour of earthen structures during the Pisco (Peru) earthquake of August 15, 2007," Proc. of the 14th World Conf. on Earthquake Engineering, No.01-1031, 2008.
[3] T. Narafu, H. Imai, S. Matsuzaki, K. Sakoda, F. Matsumura, Y. Ishiyama, and A. Tasaka, "Basic study for bridge between engineering and construction practice of non-engineered houses," Proc. of the 14th World Conf. on Earthquake Engineering, S18-003, 2008.
[4] A. S. Elnashai, H. J. Alva, O. Pineda, O. Kwon, Y. L. Moran, G. Huaco, and G. Pluta, "The Pisco-Chincha earthquake of August 15, 2007 seismological, geotechnical, and structural assessments," MAE Center Report 08-01, Mid-America Earthquake Center, Civil and Environmental Engineering Department, University of Illinois at Urbana – Champaign, IL, 2008.
[5] O. Murao and F. Yamazaki, "Development of fragility curves for buildings based on damage data due to the Hyogoken-nanbu earthquake," Proc. of the Asian-Pacific Symposium on Structural Reliability and Its Applications, pp. 259-269, 1999.
[6] K. Jaiswal, D. Wald, and D. D'Ayala, "Developing empirical collapse fragility functions for global building types," Earthquake Spectra, Vol.27, No.3, pp. 775-795, 2011.
[7] U. Hancilar, F. Taucer, and C. Corbane, "Empirical fragility functions based on remote sensing and field data after the 12 January 2010 Haiti earthquake," Earthquake Spectra, Vol.29, No.4, pp. 1275-1310, 2013.
[8] Federal Emergency Management Agency (FEMA), Multi-hazard Loss Estimation Methodology Earthquake Model (HAZUS-MH MR3), DC, 2003.
[9] N. Tarque, H. Crowley, R. Pinho, and H. Varumd, "Displacement-based fragility curves for seismic assessment of adobe buildings in Cusco, Peru," Earthquake Spectra, Vol.28, No.2, pp. 759-794, 2012.
[10] M. A. Erberik, "Generation of fragility curves for Turkish masonry buildings considering in-plane failure modes," Earthquake Engineering Structural Dynamics, Vol.37, pp. 387-405, 2008.
[11] M. A. Erberik, "Seismic risk assessment of masonry buildings in Istanbul for effective risk mitigation," Earthquake Spectra, Vol.26, No.4, pp. 967-982, 2010.
[12] National Institute of Statistic and Informatics (INEI), Census 2007, 2007.
[13] A. Sladen, H. Tavera, H. Simons, J. P. Avouac, A. O. Konca, H. Perfettini, L. Audin, E. J. Fielding, F. Ortega, and R. Cavagnoud, "Source model of the 2007 Mw 8.0 Pisco, Peru earthquake: Implications for seismogenic behavior of subduction megathrusts," Journal of Geophysical Research, Vol.115, B02405, 2010.
[14] N. Pulido, H. Tavera, Z. Aguilar, S. Nakai, and F. Yamazaki, "Strong motion simulation of the M8.0 August 15, 2007, Pisco earthquake; Effect of a multi-frequency rupture process," Journal of Disaster Research, Vol.8, No.2, pp. 235-242, 2013.
[15] C. Zavala, M. Estrada, L. Chang, L. Cardenas, J. Tayra, L. Conisla, and G. Guibovich, "Behavior of non-engineered houses during Pisco earthquake 15/8/2007," Proc. of the 14th World Conf. on Earthquake Engineering, S18-031, 2008.
[16] S. Matsuzaki, F. Yamazaki, M. Estrada, and C. Zavala, "Visual damage interpretation of buildings using QuickBird images following the 2007 Peru earthquake," Proc. of the third Asia Conf. on Earthquake Engineering, ACEE-P-067, 2010.
[17] U. S. Tejada and Buena tierra, "apuntes para el diseño y construcción con adobe," CIDAP, pp. 169, 2010 (in Spanish).
[18] Ministry of Housing, Construction and Sanitation, Peru, National Building Code (Las Normas del Reglamento Nacional de Edificaciones), E.070 Brick Structure, E.080 Adobe Structure, 2012 (in Spanish).
[19] European Macroseismic Scale 1998 (EMS-98), European Seismological Commission, G. Grünthal (editor), Luxembourg, 1998, http://www.franceseisme.fr/EMS98_Original_english.pdf [accessed Jul. 28, 2014]
[20] M. Astroza, O. Moroni, S. Brzev, and J. Tanner, "Seismic performance of engineered masonry buildings in the 2010 Maule earthquake," Earthquake Spectra, Vol.28, pp. S385-S406, 2012.
[21] M. Matsuoka and M. Estrada, "Development of earthquake-induced building damage estimation model based on ALOS/PALSAR observing the 2007 Peru earthquake," Journal of Disaster Research, Vol.8, No.2, pp. 346-355, 2013.
[22] Y. Onishi and Y. Hayashi, "Fragility curves for wooden houses considering aged deterioration of the earthquake resistance," Proc. of the 14th World Conf. on Earthquake Engineering, S12-028, 2008.
[23] J. Johansson, P. Mayorca, T. Torres, and E. Leon, Reconnaissance team by Japan Society of Civil Engineers (JSCE), Japan Association for Earthquake Engineering (JAEE) and University of Tokyo, "A reconnaissance report on the Pisco, Peru earthquake of August 15, 2007," 2007, http://www.jsce.or.jp/report/45/content.pdf [accessed Jul. 28, 2014].
[24] Y. Nakamura, "A method for dynamic characteristics estimation of subsurface using microtremor on the ground surface," Railway Technical Research Institute, Quarterly Reports, Vol.30, Issue Number 1, pp. 25-33, 1989.
[25] Y. Nakamura, "Clear identification of fundamental idea of Nakamura's technique and its applications," Proc. of the 12th World Conf. on Earthquake Engineering, pp. 2656, 2000.
[26] D. F. Watson and G. M. Philip, "A refinement of Inverse Distance Weighted interpolation," Geo-processing, Vol.2, pp. 315-327, 1985.
[27] J. P. Bardet, K. Ichii, and C. H. Lin, "EERA; A computer program for Equivalent-linear Earthquake site Response Analyses of layered soil deposits," Department of Civil Engineering, University of Southern California, CA, 2000.
[28] J. I. Sun, R. Golesorkhi, and H. B. Seed, "Dynamic moduli and damping ratios for cohesive soils," Report No. UCB/EERC-88/15, Earthquake Engineering Research Center, University of California, Berkeley, 42p., 1988.
[29] B. Mansouri, M. Ghafory-Ashtiany, K. Amini-Hosseini, R. Nourjou, and M. Mousavie, "Building seismic loss model for Tehran," Earthquake Spectra, Vol.26, No.1, pp. 153-168, 2010.

Name:
Shizuko Matsuzaki

Affiliation:
Project Researcher, Department of Urban Environment System, Graduate School of Engineering, Chiba University

Address:
1-33 Yayoi-cho, Inage-ku, Chiba 263-8522, Japan

Brief Career:
2013 Dr. Eng., Chiba University
2013 Project Researcher, Chiba University

Selected Publications:
• "Visual damage interpretation of buildings using QuickBird images following the 2007 Peru earthquake," Proc. of the third Asia Conf. on Earthquake Engineering, ACEE-P-067, 2010.

Academic Societies & Scientific Organizations:
• Architectural Institute of Japan (AIJ)
• Institute of Social Safety Science (ISSS)
• Japan Association for Earthquake Engineering (JAEE)